LETTER

doi:10.1038/nature10705

Changing Arctic Ocean freshwater pathways

James Morison[1], Ron Kwok[2], Cecilia Peralta-Ferriz[1], Matt Alkire[1], Ignatius Rigor[1], Roger Andersen[1] & Mike Steele[1]

Freshening in the Canada basin of the Arctic Ocean began in the 1990s[1,2] and continued[3] to at least the end of 2008. By then, the Arctic Ocean might have gained four times as much fresh water as comprised the Great Salinity Anomaly[4,5]of the 1970s, raising the spectre of slowing global ocean circulation[6]. Freshening has been attributed to increased sea ice melting[1] and contributions from runoff[7], but a leading explanation has been a strengthening of the Beaufort High—a characteristic peak in sea level atmospheric pressure[2,8]—which tends to accelerate an anticyclonic (clockwise) wind pattern causing convergence of fresh surface water. Limited observations have made this explanation difficult to verify, and observations of increasing freshwater content under a weakened Beaufort High suggest that other factors[2] must be affecting freshwater content. Here we use observations to show that during a time of record reductions in ice extent from 2005 to 2008, the dominant freshwater content changes were an increase in the Canada basin balanced by a decrease in the Eurasian basin. Observations are drawn from satellite data (sea surface height and ocean-bottom pressure) and *in situ* data. The freshwater changes were due to a cyclonic (anticlockwise) shift in the ocean pathway of Eurasian runoff forced by strengthening of the west-to-east Northern Hemisphere atmospheric circulation characterized by an increased Arctic Oscillation[9] index. Our results confirm that runoff is an important influence on the Arctic Ocean and establish that the spatial and temporal manifestations of the runoff pathways are modulated by the Arctic Oscillation, rather than the strength of the wind-driven Beaufort Gyre circulation.

A comparison between the results of large-scale trans-Arctic hydrographic sections in 1993 (ref. 10) and 1994 (ref. 11) and data from climatology[12] revealed a large-scale cyclonic shift in the boundary between Atlantic-derived and Pacific-derived water masses across the Arctic deep basins. This cyclonic shift was related to an increase in the cyclonic atmospheric circulation of the Northern Hemisphere associated with low Arctic sea level atmospheric pressure and characterized by an increased AO index[13] (the AO is the strength of the Northern Hemisphere Annular Mode; Supplementary Information 2).

Arctic regional indices have also been proposed to characterize Arctic Ocean change, including the doming of the sea surface characterized by the sea surface height gradient in a wind-forced model of the Arctic Ocean[6]. The doming is related to the strength of the Beaufort High and has been linked to changes in Arctic Ocean freshwater content[2,8,14], because anticyclonic wind stress drives convergence of Ekman transport in the ocean surface boundary layer, thickening the fresh surface layer and increasing the doming.

In contrast, we use a new combination of satellite altimetry and gravity, along with traditional hydrography, to show that from 2005 to 2008, an increased AO index caused the circulation to become more cyclonic and the Eurasian river runoff to be increasingly diverted eastward to the Canada basin at the expense of the Eurasian basin, with a nearly negligible increase in average Arctic Ocean fresh water.

The recent Canada basin freshening[2,4] is illustrated by *in situ* salinity observations taken in 2008 (Fig. 1) at ocean depths of 50 to 60 m that are 1–3 p.s.u. (practical salinity units, essentially equivalent to parts per thousand by weight) lower than values from pre-1990s climatology[12], a difference that is about five times the climatological root-mean-square interannual variability (Supplementary Fig. 4b). Geostrophic water velocities at 50–60 m computed from density-determined dynamic heights[15] relative to the depth where ocean pressure equals 500 dbar (1 dbar corresponds to about 1 m water equivalent pressure) for 2008 (Fig. 1) show the anticyclonic Beaufort Gyre current pattern as an intense southern core with westward motion along the Alaskan coast, but with broader eastward return flows farther north.

In contrast to the Canada basin, the Makarov basin upper-ocean salinities in 2008 are 1–2 p.s.u. greater than values from climatology[12] (Fig. 1). The corresponding trough in dynamic heights forces the geostrophic upper-ocean currents to sweep cyclonically around the southeastern part of the Makarov basin and across the Chukchi borderland (see location in Fig. 1) into the Canada basin's anticyclonic gyre.

Hydrochemistry sampling in 2008 indicates that, relative to a reference salinity of 34.87 p.s.u., Pacific water and Eurasian runoff provide the dominant fractions of freshwater in the upper 200 m of the Beaufort Sea[16]. The sea ice melt fraction is comparatively small and almost always negative, indicating the dominance of sea ice production and export over melt. We have compared spring 2008 (ref. 16) and summer 2003 (ref. 17) hydrochemistry data, and adjusting for seasonal differences[2] of the order of 1 m (Supplementary Information 3 and

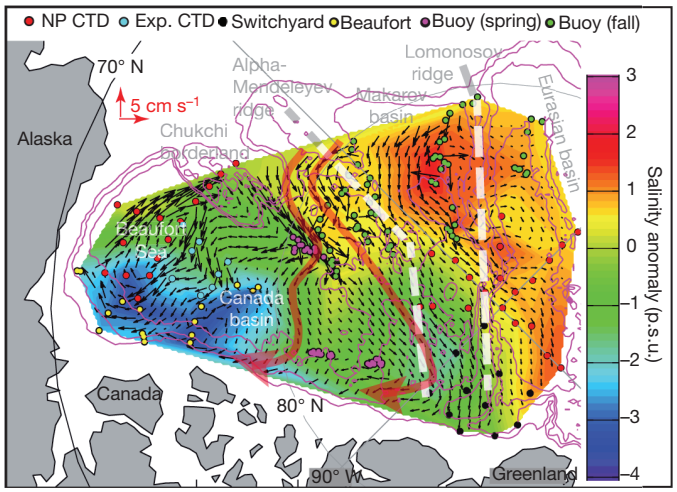

Figure 1 | 2008 Arctic Ocean salinity anomaly and geostrophic velocity at 50–60 m depth. The salinity anomaly (colour shading) is relative to the pre-1990 winter climatology[12] given in practical salinity units. The velocities (vectors) are derived from dynamic heights relative to the 500-dbar pressure surface[15]. Red arrows highlight S-shaped pathways from the Russian shelves into the Canada basin anticyclonic gyre. Dashed lines highlight the Alpha-Mendeleyer and Lomonosor ridges. 'NP CTD', 'Exp. CTD' and 'Switchyard' are the hydrographic stations done in spring 2008, 'Beaufort' represents the hydrographic stations done in summer 2007, and 'Buoy (spring)' and 'Buoy (fall)' indicate hydrographic data[15] from Ice Tethered Profilers gathered in autumn 2007 and spring 2008.

[1]Polar Science Center, Applied Physics Laboratory, University of Washington, 1013 Northeast 40th Street, Seattle, Washington 98105, USA. [2]Jet Propulsion Laboratory, California Institute of Technology, 4800 Oak Grove Drive, Pasadena, California 91109, USA.

Supplementary Figs 5 and 6), we find that the change in average freshwater inventories in the top 195 m of the Beaufort Sea are 0.6 m of sea ice melt, −0.8 m of Pacific water and 3.6 m of Eurasian runoff, with a total increase of 3.4 m. Only the increases in Eurasian runoff and the total inventories are substantially greater than the standard errors (s.e.) of these averages, owing to the variability among stations (s.e. value is 0.93 m for sea ice melt, 0.3 m for Pacific water and 0.99 m for Eurasian runoff, with an s.e. value for the total of 1.12 m; see Supplementary Information 3). From 2003 to 2008, the dominant source of freshening is increased Eurasian runoff, especially in the depth range of 50 to 115 m (Supplementary Information 3 and Supplementary Fig. 5), consistent with transport by geostrophic currents extending down into the upper halocline that come cyclonically around the Makarov basin into the Canada basin (Fig. 1).

Combined with spot verification by hydrography[15,16], dynamic ocean topography (DOT, deviation of the sea surface from the geoid) from the Ice Cloud and Land Elevation Satellite (ICESat) laser altimeter[15] and ocean bottom pressure (OBP) from the Gravity Recovery and Climate Experiment Gravity (GRACE) satellites (Supplementary Information 4) provide the spatial and temporal coverage needed to understand the 2005–2008 Arctic Ocean changes. OBP is the sum of DOT and the steric pressure anomaly (SPA, due to changes in water density). Comparisons among satellite-derived DOT and OBP and *in situ* observations of SPA have been done for temperate oceans[18,19], but this is the first such effort for the Arctic Ocean. Models indicate that at shorter than seasonal timescales, Arctic OBP variations are barotropic (Supplementary Information 4) and reflect DOT variations[20,21]. At interannual and longer timescales the deep ocean response is baroclinic, OBP variations are smaller than DOT variations, and the SPA is comparable to −DOT (Supplementary Fig. 7). Comparisons of ICESat DOT with hydrography[15] (Supplementary Information 4) and with GRACE OBP confirm this for the Arctic Ocean; multiyear variations in DOT, with a fractional correction by OBP, yield the multiyear variations in SPA.

DOT from 2005 to 2008 increased at ~5–8 cm yr^{-1} (uncertainty is standard deviation (s.d.) of 0.9 cm yr^{-1}; Supplementary Information 4) in the Canada basin (Fig. 2a), resulting in anticyclonic spin-up of the surface velocity. However, DOT decreased by 3−4 cm yr^{-1} in a trough aligned with the Eurasian continental shelf-break (seaward edge of the shallow continental shelf), resulting in increasing DOT-gradient-driven eastward surface velocities and transport of Eurasian river water along the Russian shelf. Variations in the pattern include cyclonic cells that allow for the runoff-rich coastal water to be carried across the shelf and into the eastern Makarov basin and Chukchi borderland regions. Furthermore, the increase in DOT towards the Russian coast could be driving a seaward secondary flow in the bottom boundary layer over the shelf that injects runoff-enriched water into the upper halocline of the central basin, where we find increases in the Eurasian runoff.

ICESat DOT rates of change agree with those inferred from the difference between GRACE OBP and the SPA from repeat hydrographic stations (Fig. 2a, correlation 0.84, for number of samples $N = 19$; 99% confidence limits: 0.5 < correlation coefficient < 0.95); the s.d. of DOT relative to OBP minus DOT, 1.2 cm yr^{-1}, is also applicable to SPA rate of change from the difference between GRACE OBP and ICES at DOT rates of change (Supplementary Fig. 10). Taking the difference of the DOT and OBP rates of change (Supplementary Information 4, OBP 4-year, 42-sample, rate-of-change uncertainty= ±0.37 cm yr^{-1}; ref. 22) yields estimates of SPA changes over the whole Arctic Ocean (Fig. 2b)—to our knowledge the first such estimates. The increasing SPA (3–5 cm yr^{-1}) in the Eurasian basin and along the Russian shelf-break balances the decreasing (−4 to −6 cm yr^{-1}) SPA in the Canada basin associated with declining salinity.

SPA is negatively related to freshwater content in cold polar oceans[23]. The correlation of SPA and freshwater content calculated directly for the Beaufort Sea (Supplementary Fig. 12) suggests that

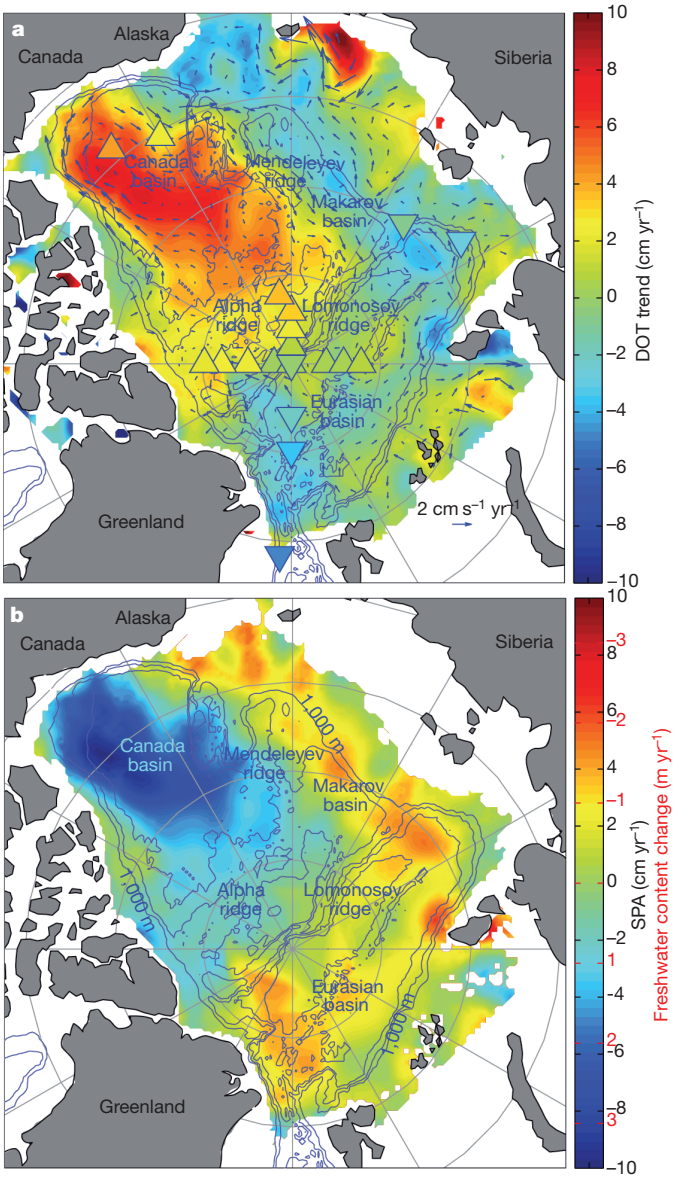

Figure 2 | Rates of change between 2005 and 2008 of DOT, SPA and freshwater content. **a**, DOT rate of change from ICESat altimetry (s.d. 0.9 cm yr^{-1}, Supplementary Information 4). Arrows show rate of change in near-surface velocity driven by DOT. The DOT rate of change equal to GRACE OBP rate of change minus SPA rate of change from hydrography are shown as colour-coded triangles (s.d. of difference is 1.2 cm yr^{-1}, Supplementary Fig. 10). **b**, SPA rate of change (±1.2 cm yr^{-1}) equal to the OBP rate of change (Supplementary Fig. 9) minus the DOT rate of change (Fig. 2a) for water depths over 50 m (Supplementary Information 5). The scale labelled in red indicates the change in freshwater content, −35.6 × SPA (±0.42 m yr^{-1}, Supplementary Information 6).

freshwater content is approximately −35.6 × SPA (Fig. 2b). Freshwater content changes are dominated by strong increases in the Canada basin balanced by decreases in the Eurasian basin and along the Russian shelf-break, reflecting change in Eurasian runoff pathways.

The area-averaged 2005–2008 freshwater rate of change (Fig. 2b) of 0.04 m yr^{-1} is almost insignificant (s.e. 0.034 m yr^{-1}, Supplementary Information 6). If we consider the deep basin only (water depths exceeding 500 m), the average is greater at 0.18 m yr^{-1} (s.e. 0.039 m yr^{-1}, Supplementary Information 6), because the 500-m depth contour runs near the middle of the freshwater minimum along the Russian shelf-break (Fig. 2b). This is essentially equal to the rate of change estimated for the deep basin over the previous decade[3]. The

rate of change of deep-basin freshwater volume and its difference from the larger area average are comparable to recent rates of change in ice volume[24] and variations in liquid freshwater exports[25] (Supplementary Information 7), illustrating the importance of observations with sufficiently broad spatial coverage (Supplementary Information 9).

Maps of 2006–2008 sea level pressure (SLP), DOT and SPA anomalies (Fig. 3) are consistent with variations in the AO. Just as highs in SLP force convergence of near-surface Ekman transport, doming of DOT and deepening of isohaline surfaces, SLP lows cause divergence, development of a trough in DOT and shoaling of isohalines. Whereas the Beaufort High dominates the mean SLP pattern, the AO manifests itself over the Arctic Ocean as a trough of low pressure extending from the Greenland–Norwegian seas into the Eurasian and Makarov basins (Supplementary Fig. 2). When the winter AO index increased in 2007, the SLP anomaly decreased over the Eurasian and Makarov basins, reflecting the AO pattern (Fig. 3a). The trough in SLP anomaly forces a trough in DOT aligned with the Russian shelf-break (Fig. 3b and Fig. 2a). The trough pattern includes upwelling of isohaline surfaces under the centre of the trough, as indicated by increased SPA (Fig. 3c, Fig. 2b). It also includes increased DOT and downwelling of isohalines across the Russian shelf. Raised DOT towards the coast moves fresher runoff-rich water eastward. The average upper-ocean circulation patterns for 2004–2005 (Supplementary Fig. 13e) and 2007–2009 (Supplementary Fig. 13f) confirm in absolute terms the increased cyclonic circulation on the Russian side of the Arctic Ocean (Figs 2a and 3b).

Our observations suggest idealized modes of Arctic Ocean circulation (Fig. 4). In the low-AO-index mode (Fig. 4a), an expanded high in SLP drives an anticyclonic surface circulation over most of the basin. The SLP pattern is similar to the mean SLP pattern (Supplementary Fig. 2a) but strengthened and expanded westward. Eurasian runoff leaves the Arctic directly across the Eurasian basin. In the high-AO-index pattern (Fig. 4b), cyclonic motion occurs on the Russian side of the Arctic Ocean, and the anticyclonic cell shifts to the southeast in the Canada basin. Eurasian runoff is diverted eastward and off the East Siberian shelf into the Canada basin circulation, where it can increase freshwater content through Ekman transport at the surface and by geostrophic currents at depth. The dipole character of the cyclonic mode and its connection to the AO cannot be captured by the doming index[6] because the doming criterion considers only a single DOT feature.

The 2005–2008 high-AO-index shift exemplifies a change in Arctic Ocean characteristics that began in 1989 and largely characterized the next 20 years (Supplementary Information 2). Then, as in 2005–2008, the AO index increased relative to its pre-1989 average, and the transpolar drift of sea ice and surface water shifted cyclonically[10] (Supplementary Fig. 13a–f). Salinity increased in the Makarov and Eurasian basins[10,26,27] and decreased in the Beaufort Sea[1,2] (Supplementary Fig. 4a) owing to an increase in the fraction of runoff[7], specifically caused by a diversion of Eurasian runoff to the east[26,27]. An important difference is that, although the 2005–2008 Canada basin circulation was increasingly anticyclonic, it became less anticyclonic and doming decreased in the early 1990s[2] (Supplementary Figs 13a–f). Clearly, increased doming was not the cause of the 1990s Beaufort Sea freshening.

The climate implications of cyclonic AO-induced shifts in freshwater pathways include increasing deep thermohaline convection in

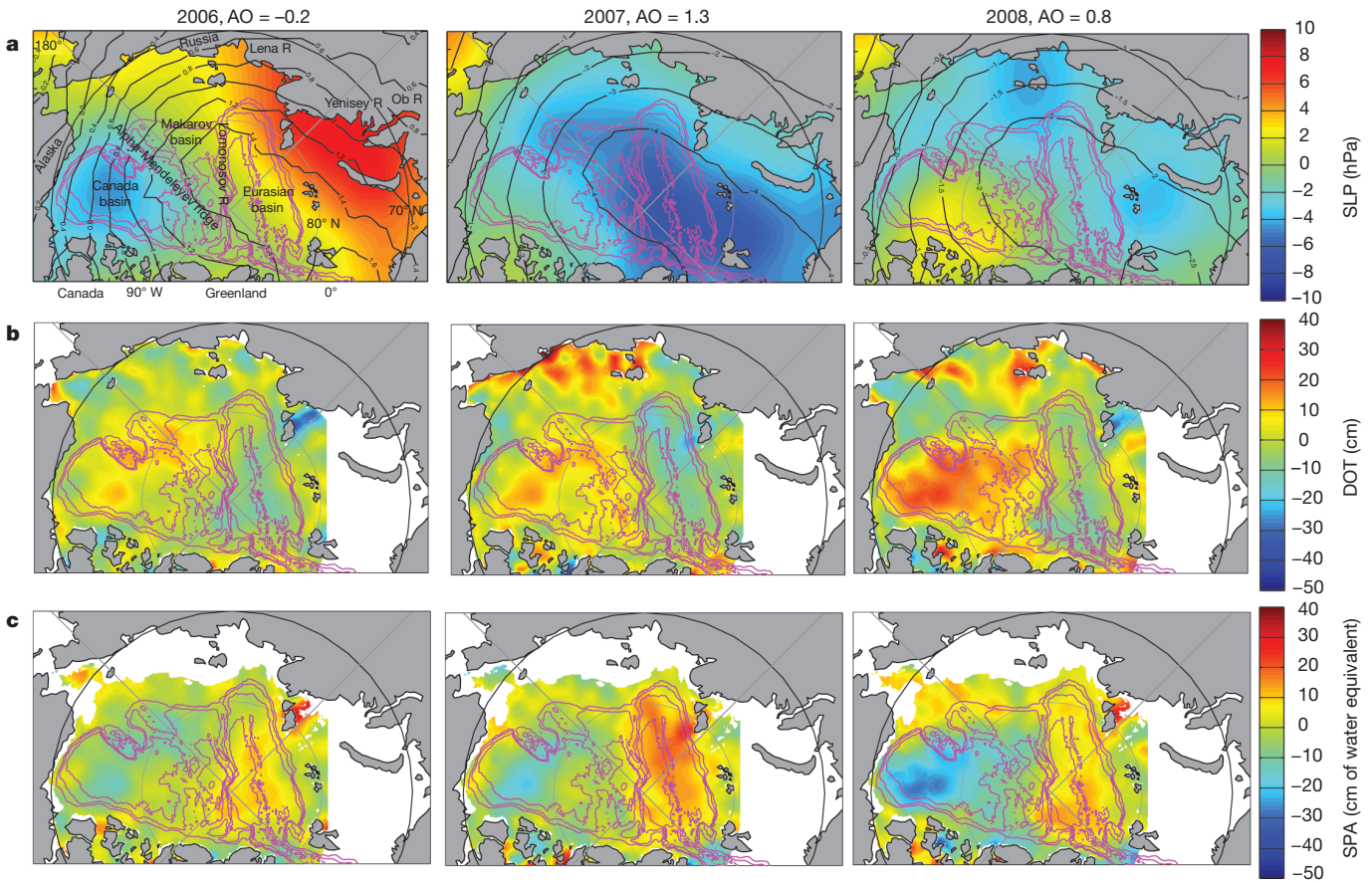

Figure 3 | 2006–2008 anomalies relative to 2004–2005 averages of SLP, DOT and SPA. **a**, Winter sea level atmospheric pressure from the International Arctic Buoy Program (http://iabp.apl.washington.edu/data_slp.html). Black contours are the mean SLP anomaly relative to 2004–2005 plus the AO contribution. **b**, DOT (February–March) (in cm). **c**, SPA, equal to the February–March-average OBP minus DOT. The SLP is the winter (previous November–April) average. The text AO value is the winter (November–April) average anomaly relative to the 1950–1989 average winter AO.

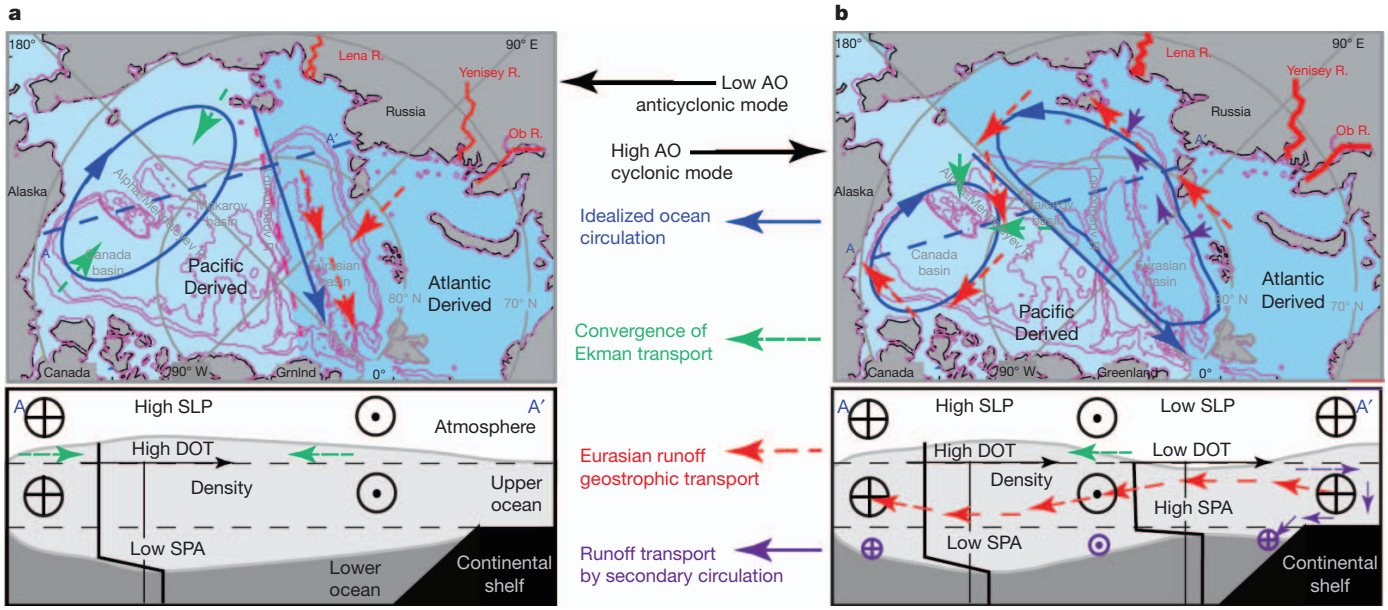

Figure 4 | Schematic views of the idealized Arctic Ocean circulation patterns under low and high AO anomalies. At the top are plan views and at the bottom are section views for the anticyclonic pattern for low AO index (**a**) and the cyclonic pattern for high AO index (**b**). The blue arrows indicate the prevailing surface geostrophic ocean circulation. The Ob, Yenisey and Lena rivers are the dominant sources of runoff to the Arctic Ocean. The red, green and purple arrows show the Eurasian runoff freshwater paths as indicated.

the Greenland Sea at the expense of the Labrador Sea, and enhancing sea ice melt by weakening the cold halocline layer of the Eurasian basin[27]. Climate models suggest an increasing AO with greenhouse warming[28], but the atmospheric models used typically produce low-pressure anomalies centred over the central Arctic Ocean[28–30] or show a negative AO bias[30] (Supplementary Information 1). Climate models need to capture the asymmetric effect of the AO on SLP in the Arctic to predict the role of the Arctic Ocean in our changing climate.

METHODS SUMMARY

The 2005–2008 repeat hydrographic stations (Figs 2 and 3) are from the North Pole Environmental Observatory (NPEO, http://psc.apl.washington.edu/northpole/) and Lincoln Sea Switchyard (http://psc.apl.washington.edu/switchyard/index.html) airborne surveys, plus the Beaufort Gyre Exploration Project (http://www.whoi.edu/beaufortgyre/) ship-borne surveys. Data from near the Laptev Sea shelf-break are from the Nansen and Amundsen Basin Observational System (http://nabos.iarc.uaf.edu/) and Fram Strait data comes from the Norwegian Polar Institute (http://www.npolar.no/en/).

The spring 2008 NPEO programme (Fig. 1) included conductivity–temperature–depth and hydrochemistry (Supplementary Information-3) stations in the North Pole and Beaufort Sea regions[4,16] augmented by Ice Tethered Profile buoy conductivity–temperature–depth data (http://www.whoi.edu/science/PO/arcticgroup/projects/ipworkshop.html). For Fig. 1, salinity anomalies and dynamic heights relative to 500 dbar at each station are linearly interpolated, and the gradients in dynamic height determine geostrophic currents[15].

We use GRACE monthly fields of OBP from the University of Texas Center for Space Research release 4 (dpc201012), from August 2002 to December 2009 (http://grace.jpl.nasa.gov/data) processed from spherical harmonic gravity coefficients by the Center for Space Research following ref. 31. The values represent anomalies relative to the mean from January 2003 to December 2007. We use data filtered with a 300-km half-amplitude radius Gaussian smoother. The GRACE Arctic OBP has been validated with *in situ* pressure at the North Pole[22].

We derive DOT (here filtered with a 100-km radius Gaussian smoother) as the difference between ICESat laser altimeter measurements of sea surface height in open water leads relative to the WGS84 ellipsoid and the EGM2008 geoid[15]. These data are available for download at http://rkwok.jpl.nasa.gov/icesat/data_topography.html. The DOT measured with ICESat in February–March 2008 are well correlated (correlation coefficient, $r_{corr} = 0.92$, $N = 176$, 99% confidence limits: $0.884 < r_{corr} < 0.945$) with dynamic height relative to 500 dbar calculated from 2008 hydrographic data (Supplementary Fig. 8). The resulting geostrophic surface velocities show the same features derived from the dynamic heights relative to 500 dbar (Fig. 1)[15].

Received 9 February; accepted 9 November 2011.

1. McPhee, M. G., Stanton, T. P., Morison, J. H. & Martinson, D. G. Freshening of the upper ocean in the Arctic: is perennial sea ice disappearing? *Geophys. Res. Lett.* **25,** 1729–1732 (1998).
2. Proshutinsky, A. *et al.* Beaufort Gyre freshwater reservoir: state and variability from observations. *J. Geophys. Res.* **114,** C00A10, http://dx.doi.org/10.1029/2008JC005104 (2009).
3. Rabe, B. *et al.* An assessment of Arctic Ocean freshwater content changes from the 1990s to the 2006–2008 period. *Deep Sea Res. I* **58,** 173–185 (2011).
4. McPhee, M. G., Proshutinsky, A., Morison, J., Steele, M. & Alkire, M. Rapid change in freshwater content of the Arctic Ocean. *Geophys. Res. Lett.* **36,** L10602, http://dx.doi.org/10.1029/2009GL037525 (2009).
5. Dickson, R. R., Meincke, J., Malmberg, S. A. & Lee, A. J. The 'Great Salinity Anomaly' in the northern North Atlantic 1968–1982. *Prog. Oceanogr.* **20,** 103–151 (1988).
6. Proshutinsky, A. Y. & Johnson, M. A. Two circulation regimes of the wind-driven Arctic Ocean. *J. Geophys. Res.* **102,** 12493–12514 (1997).
7. Macdonald, R. W., Carmack, E. C., McLaughlin, F. A., Falkner, K. K. & Swift, J. H. Connections among ice, runoff and atmospheric forcing in the Beaufort Gyre. *Geophys. Res. Lett.* **26,** 2223–2226 (1999).
8. Proshutinsky, A., Bourke, R. H. & McLaughlin, F. A. The role of the Beaufort Gyre in Arctic climate variability: seasonal to decadal climate scales. *Geophys. Res. Lett.* **29,** 2100, http://dx.doi.org/10.1029/2002GL015847 (2002).
9. Thompson, D. W. J. & Wallace, J. M. The Arctic Oscillation signature in the wintertime geopotential height and temperature fields. *Geophys. Res. Lett.* **25,** 1297–1300 (1998).
10. Morison, J., Steele, M. & Andersen, R. Hydrography of the upper Arctic Ocean measured from the nuclear submarine USS Pargo. *Deep Sea Res. I* **45,** 15–38 (1998).
11. Carmack, E. C. *et al.* Changes in temperature and tracer distributions within the Arctic Ocean: results from the 1994 Arctic Ocean Section. *Deep Sea Res. II* **44,** 1487–1502 (1997).
12. Environmental Working Group (EWG). *Joint U.S.-Russian Atlas of the Arctic Ocean, Oceanography Atlas for the Winter Period* (National Ocean Data Center (NODC), 1997).
13. Morison, J., Aagaard, K. & Steele, M. Recent environmental changes in the Arctic. *Arctic* **53,** 359–371 (2000).
14. Lique, C. *et al.* Evolution of the Arctic Ocean Salinity, 2007–08: contrast between the Canadian and the Eurasian Basins. *J. Clim.* **24,** 1705–1717 (2011).
15. Kwok, R. & Morison, J. Dynamic topography of the ice-covered Arctic Ocean from ICESat. *Geophys. Res. Lett.* **38,** L02501, http://dx.doi.org/10.1029/2010GL046063 (2011).
16. Alkire, M. B. *et al.* Sensor-based profiles of the NO parameter in the central Arctic and southern Canada Basin: new insights regarding the cold halocline. *Deep Sea Res. I* **57,** 1432–1443 (2010).
17. Yamamoto-Kawai, M., McLaughlin, F. A., Carmack, E. C., Nishino, S. & Shimada, K. Freshwater budget of the Canada Basin, Arctic Ocean, from salinity, $\delta^{18}O$, and nutrients. *J. Geophys. Res.* **113,** C01007, http://dx.doi.org/10.1029/2006JC003858 (2008).

18. Chambers, D. P. Observing seasonal steric sea level variations with GRACE and satellite altimetry. *J. Geophys. Res.* **111,** C03010, http://dx.doi.org/10.1029/2005JC002914 (2006).
19. Willis, J. K., Chambers, D. P. & Nerem, R. S. Assessing the globally averaged sea level budget on seasonal to interannual timescales. *J. Geophys. Res.* **113,** C06015, http://dx.doi.org/10.1029/2007JC004517 (2008).
20. Vinogradova, N., Ponte, R. M. & Stammer, D. Relation between sea level and bottom pressure and the vertical dependence of oceanic variability. *Geophys. Res. Lett.* **113,** L03608, http://dx.doi.org/10.1029/2006GL028588 (2007).
21. Bingham, R. J. & Hughes, C. W. The relationship between sea-level and bottom pressure variability in an eddy permitting ocean model. *Geophys. Res. Lett.* **35,** L03602, http://dx.doi.org/10.1029/2007GL032662 (2008).
22. Morison, J., Wahr, J., Kwok, R. & Peralta-Ferriz, C. Recent trends in Arctic Ocean mass distribution revealed by GRACE. *Geophys. Res. Lett.* **34,** L07602, http://dx.doi.org/10.1029/2006GL029016 (2007).
23. Steele, M. & Ermold, W. Steric sea level change in the Northern Seas. *J. Clim.* **20,** 403–417 (2007).
24. Kwok, R. *et al.* Thinning and volume loss of the Arctic Ocean sea ice cover: 2003–2008. *J. Geophys. Res.* **114,** C07005, http://dx.doi.org/10.1029/2009JC005312 (2009).
25. Serreze, M. C. *et al.* The large-scale freshwater cycle of the Arctic. *J. Geophys. Res.* **111,** C11010, http://dx.doi.org/10.1029/2005JC003424 (2006).
26. Ekwurzel, B., Schlosser, P., Mortlock, R. A., Fairbanks, R. G. & Swift, J. H. River runoff, sea ice meltwater, and Pacific water distribution and mean residence times in the Arctic Ocean. *J. Geophys. Res.* **106,** 9075–9092 (2001).
27. Steele, M. & Boyd, T. Retreat of the cold halocline layer in the Arctic Ocean. *J. Geophys. Res.* **103,** 10419–10435 (1998).
28. Shindell, D. T., Miller, R. L., Schmidt, G. A. & Pandolfo, L. Simulation of recent northern winter climate trends by greenhouse-gas forcing. *Nature* **399,** 452–455 (1999).
29. Koldunov, N. V., Stammer, D. & Marotzke, J. Present-day Arctic sea ice variability in the coupled ECHAM5/MPI-OM model. *J. Clim.* **23,** 2520–2543 (2010).
30. Walsh, J. E., Chapman, W. L., Romanovsky, V., Christensen, J. H. & Stendel, M. Global Climate Model performance over Alaska and Greenland. *J. Clim.* **21,** 6156–6174 (2008).
31. Chambers, D. P. Evaluation of new GRACE time-variable gravity data over the ocean. *Geophys. Res. Lett.* **33,** L17603 (2006).

Supplementary Information is linked to the online version of the paper at www.nature.com/nature.

Acknowledgements This work was supported chiefly by NSF grants OPP 0352754, ARC-0634226, ARC-0856330 and NASA grant NNX08AH62G. R.K. was supported at the Jet Propulsion Laboratory, California Institute of Technology, under contract with NASA. GRACE ocean data were processed by D. P. Chambers, supported by the NASA MEASURES Program. We thank the NASA ICESat and GRACE programmes, K. Falkner, R. Collier, M. McPhee, W. Ermold, L. de Steur, A. Proshutinsky and the Beaufort Gyre Exploration Project, J. Toole and R. Krishfield and the Ice Tethered Profiler project at WHOI, and W. Smethie of the Switchyard project for the observations that made this work possible.

Author Contributions The main idea was developed by J.M. and R.K. J.M. wrote most of the text and with R.A. and C.P.-F. drew most of the figures. R.K. developed the DOT records. The SLP and OBP anomaly plots were originally developed by C.P.-F. The 2008 hydrography observations were made by J.M., M.A., R.A. and M.S. The AO spatial pattern data, figures and insight were provided by I.R. The hydrographic data processing was done by R.A. and the chemistry analysis was done by M.A. Switchyard data and freshwater insight was provided by M.S. All authors discussed the results and commented on the manuscript.

Author Information Reprints and permissions information is available at www.nature.com/reprints. The authors declare no competing financial interests. Readers are welcome to comment on the online version of this article at www.nature.com/nature. Correspondence and requests for materials should be addressed to J.M. (morison@apl.washington.edu).